DEVELOPMENT OF IN-SITU MEASUREMENTS TO DETERMINE RESERVOIR CONDITION CRITICAL GAS SATURATIONS DURING DEPRESSURISATION

Peter Naylor, David Mogford and Robert Smith
AEA Technology plc

ABSTRACT

This paper describes the development of experimental methods to determine critical gas saturations and relative permeabilities relevant to the depressurisation of volatile oils. A series of reservoir condition coreflood experiments at pressures up to 415 bara and 123°C is described. The experiments were conducted with aged core and fluids and comprised of a waterflood followed by depressurisation at different rates. A key part of the laboratory data was the measurement of extensive three-phase in-situ saturations. These measurements were conducted at full reservoir conditions by adding discrete gamma-emitting radioactive tracers to the brine and oil phases.

The experiments were complicated by the following features and successful solutions have been implemented:

- high CO_2 content of the oil
- radioactive tracer adsorption on the rock
- ultra-low flow rates

The oil contained up to 22 mole% CO_2 and compatibility trials were conducted with the gamma-emitting radioactive tracers. The oil phase tracer was ferrocene ($C_{10}H_{10}Fe$) containing iron-59 (Fe^{59}), and the initial brine phase tracer was potassium cobalticyanide ($K_3Co[CN]_6$) containing cobalt-58 (Co^{58}). The $C_{10}H_{10}Fe$ was demonstrated to be compatible, but the initial brine phase tracer was replaced with caesium chloride (CsCl) containing caesium-137 (Cs^{137}).

This Cs^{137} brine phase tracer adsorbed on the core and the magnitude of the adsorption was a function of the experimental conditions. It was necessary to calibrate the tracers at reservoir conditions and this required the development of a new flooding protocol and the measurement of in-situ porosity using a gamma-attenuation technique.

In order to investigate the influence of depressurisation rate on critical gas saturation, a range of rates was investigated. The longest duration experiment involved depressurisation over a period of 141 days with an average flow rate of just 0.3 mL day^{-1}. This low rate required extremely high standards of leak integrity. It was necessary to develop a new core sleeving arrangement that combined low gamma-attenuation with ultra-high leak tightness. The high CO_2 content did not favour the use of elastomer or epoxy resin coated cores during depressurisation, and a core sleeve involving PTFE and aluminium was developed. Produced fluids were collected at reservoir conditions in a visual cell and the very low flow rates could not overcome the static friction of the piston in the visual cell. This problem was solved with the novel use of a fluorinated hydrocarbon which acted as a 'liquid-piston'.

The development of new experimental procedures has enabled the measurement of three-phase, in-situ saturations during the depressurisation of volatile oils. This data has been used to determine critical gas saturations and derive relative permeabilities which can be used in reservoir simulations.

1.   INTRODUCTION

Estimation of recoverable reserves and the management of reservoir performance usually require measurement of relative permeability data, but unfortunately, unless studies are carefully conducted this data can be of dubious quality and/or relevance to the development decisions under consideration. We are exhorted to have an "integrated and rigorous approach to SCAL data management because the net present value of the total field development project is at risk in direct proportion to the possibility of measurement uncertainty" [1]. The question that faces the SCAL community is how can we generate cost effective data relevant to field management decisions? We can learn much from analogue studies, but many processes are such that there is no substitute for full reservoir condition experiments. In other words getting the right fluids in the right place in the right core and thus ensuring the correct balance of gravity, viscous and capillary forces. Key parameters include:

- Rock
- Fluids
- Pressure and temperature
- Fluid/fluid/rock interactions

- Fluid distribution/flow regime
- Flow direction
- Flow rate
- Length scale

It is now possible to conduct experiments in which the first seven parameters approach field conditions for many reservoir processes. By its very nature, length scale is always going to be a challenge for laboratory experiments and we are faced with two questions. Firstly, can we allow for the impact of core artifacts relating to capillary end effects and secondly, can we upscale the data for use in reservoir simulation.

This paper describes what may be the most representative depressurisation experiments that have been conducted to date. Great effort has been expended in ensuring that the key parameters were correctly represented in the reservoir condition experiments. Particular challenges related to the high CO_2 content of the oil and the low flow rates anticipated during these studies. In order to assess the impact of core artifacts and generate relative permeability data, three-phase in-situ saturation measurements have been conducted.

All too often results are reported without the detailed "how" which is a critical part of understanding the data [2]. This paper attempts to redress the balance and focuses on the development of experimental methods which have been used to examine the depressurisation of volatile oils. An overview of the results is given in Section 2 and further details are given in Reference 3. This work was part of a larger study and the overall aims are described in Reference 4.

2.   EXPERIMENTAL OVERVIEW

2.1   Core and Fluid Selection

Three experiments have been conducted for the BP Amoco Miller field and one experiment for the Marathon South Brae field. Each operator provided a selection of cores. In order to obtain an acceptably large pore volume it was necessary to butt two cores together. The cores for each assembly were selected on the basis of matching porosity, absolute permeability and pore size distribution.

There was concern relating to the possibility of calcium carbonate scaling during the depressurisation and although this may be an issue in some development plans, it was decided that it might obscure the fundamental mechanisms associated with depressurisation. The decision was taken to make synthetic formation brines without the calcium, and modified brine recipes were supplied by the operators. In order to facilitate the in-situ saturation measurements, a radioactive tracer was added to the brine.

Neither bottom hole fluids, nor separator gas was available for use in these experiments and so the live oil was made from stock tank oil and synthetic gas together with a radioactive tracer.

2.2 Conditioning

Before each experiment, the core assembly was given a mild clean with alternating toluene/methanol flushes and then flooded to 100% brine at ambient conditions. The core was then flooded to connate brine in a vertically downward direction with a 21 cp paraffin at ambient temperature. The inlet pressure was maintained at 2.7 bara with an ambient outlet pressure. Following breakthrough, the inlet pressure was gradually increased to 9.6 bara and flooding was continued until brine production effectively ceased and a near connate saturation had been achieved. In all cases, the in-situ saturation measurements demonstrated that the brine distribution was reasonably uniform throughout the core and the final brine saturations were similar to field values.

The paraffin was removed by injecting kerosene which acted as a buffer between the paraffin and live oil. The pressure and temperature were then raised to reservoir conditions whilst maintaining a net overburden pressure of 69 bar. The kerosene was displaced by inactive live oil and the core was aged for an extended period of time. The live oil was refreshed during the ageing period and towards the end, the inactive live oil was displaced by active live oil. Oil permeabilities at connate brine were determined.

2.3 Core Flooding

A waterflood was conducted by supplying active live brine to the bottom of the vertical core at constant pressure and extracting fluids from the top of the core at constant flow rate. Throughout the experiments, pressures, flow rates, produced fluid volumes and in-situ saturations were measured.

The depressurisation was conducted by isolating the bottom of the core and continuously extracting fluids from the top of the core. In Experiments 1 and 2 fluids were extracted at a constant flow rate and in Experiment 3 and 4 the flow rate was adjusted to give a linear pressure decline with time.

2.4 Experimental Data

A summary of the key parameters and results of Experiments 1-4 is given in Table 1 below:

Table 1: Key Experimental Parameters and Results

Parameter	Experiment 1	Experiment 2	Experiment 3	Experiment 4
Field	Miller	Miller	Miller	South Brae
Type of rock	Sandstone	Sandstone	Sandstone	Conglomerate
Length of core assembly (mm)	355	515	515	428
Diameter (mm)	37.8	37.8	37.8	37.8
Porosity	0.155	0.208	0.208	0.119
Pore Volume (mL)	61.7	120.5	120.5	56.9
Absolute permeability (mD)	27	492	493	292
Brine phase tracer	Co^{58}	Cs^{137}	Cs^{137}	Cs^{137}
Connate brine saturation	0.33	0.27	0.24	0.23
Temperature (°C)	120	120	120	123
Conditioning pressure (bara)	415	415	415	311
Depressurisation start pressure (bara)	368	370	357	279
Bubble point pressure (bara)	338	340	340	254
Ageing period (days)	64	20	57	94
Waterflood residual oil saturation	0.48	0.27	0.30	0.28
Mean depressurisation rate (bar/day)	52.7	6.10	1.82	6.79
Depressurisation duration (days)	5.3	47.0	140.5	30.5

Critical gas saturations were measured in the range of 0.03 to 0.21

Further details and a discussion of the results from Experiments 1-3 are given in Reference 3. The remaining sections of this paper outline the development of the experimental methods that were required to generate this data and are illustrated using results from Experiment 4.

3. IN-SITU SATURATION MEASUREMENTS

3.1 Introduction

Three-phase in-situ saturation measurements have been conducted throughout these experiments using a gamma-emission technique which involved labelling the oleic and aqueous phases with radioactive tracers. This method has been used routinely by AEA Technology for nearly twenty years and is described more fully in References 5 and 6. Fe^{59} in the form of $C_{10}H_{10}Fe$ was used as the hydrocarbon phase tracer. Initially Co^{58} in the form of $K_3Co[CN]_6$ and latterly Cs^{137} in the form of $CsCl$ was used as the brine phase tracer. The characteristic gamma energy spectra of the Fe^{59} and Co^{58}/Cs^{137} isotopes are distinct and the intensity of each spectrum was measured using a multi-channel analyser connected to a pair of 76 mm diameter sodium iodide detectors located inside a collimated lead housing. The detectors were mounted 300 mm apart vertically above one another and each had a spatial resolution of approximately 30 mm. The detectors were moved along the whole length of the core assembly using a stepper motor under computer control and measurements were made at 30 mm intervals commensurate with the spatial resolution. The data was then analysed to determine the intensity of the gamma-ray emissions and hence respective fluid saturations.

This paper, together with Reference 3, is believed to be the first unclassified publication of reservoir condition, three-phase, in-situ saturation measurements to date and these measurements were essential for identifying laboratory artifacts and determining the critical gas saturations and relative permeabilities.

3.2 Fluid Compatibility

Previous experiments with $C_{10}H_{10}Fe$ and $K_3Co[CN]_6$ have found that these radiotracers readily dissolved in reservoir fluids and no compatibility problems were observed. The level of adsorption was also found to be acceptable. However, because the reservoir fluids used in this series of depressurisation experiments had concentrations of CO_2 as high as 22 mole%, some concern was raised over the compatibility of the $C_{10}H_{10}Fe$ tracer.

Dynamic filtration trials were performed with $C_{10}H_{10}Fe$ dissolved in the reservoir fluids to see if there were any problems including decomposition leading to precipitation, which could affect the core or measurement. The results indicated that the $C_{10}H_{10}Fe$ was not affected by these high concentrations of CO_2.

During Experiment 1 difficulty was experienced with the $K_3Co[CN]_6$ tracer. There was significant adsorption combined with precipitation of some of the salts in the brine. Following investigation, it was concluded that the high levels of CO_2 in the brine caused a reduction in the pH and significantly increased corrosion of the Firth-Vickers stainless steel vessel in which the active brine was stored. The corrosion products included an insoluble complex containing Co^{58} which precipitated out. This reduced the specific activity of the brine and resulted in some fixed activity at the core inlet. A new brine storage vessel made from corrosion resistant Hastelloy was used in Experiments 2-4 to eliminate any reaction between the brine and the storage vessel.

Following the problems experienced with $K_3Co[CN]_6$ an alternative brine tracer, $CsCl$ labelled with Cs^{137} was identified. Cs^{137} fulfilled the key selection criteria that the tracer should emit gamma-rays with energies that were significantly different from those emitted by Fe^{59}. Flooding trials were performed using reservoir core and brine containing the radioactive $CsCl$ and CO_2 to assess compatibility. The trials were conducted at 100°C and 9 bara, and indicated that the $CsCl$ was compatible with the brine, but there was some adsorption of the tracer on the core.

3.3 Tracer Adsorption

The level of Cs^{137} adsorption was equivalent to a brine saturation of 0.11 and this was considered to be acceptable if it remained at a fixed level. The in-situ brine saturation measurements could be calibrated to remove the effect of the adsorption by reference to the produced fluid data. It was believed that the adsorption process was 'dynamic' and the ratio of active/inactive adsorption was a function of the ratio of active/inactive tracer in the brine. In an attempt to minimise potential adsorption, the core was pre-flooded with brine containing a similar concentration of inactive CsCl and the ratio of active/inactive tracer was 1/2467.

During the conditioning of the core in Experiment 2, it was flooded with 100% inactive degassed brine at ambient conditions and then flooded with 100% active degassed brine. The brine pH was measured to be 8.5. The variation of activity at the outlet of the core indicated that the level of adsorption was significantly higher that that observed in the trial and was equivalent to a brine saturation of 1.83. During the reservoir condition secondary waterflood the adsorption was observed to significantly reduce and extensive flooding was required to ensure a new stable level of adsorption had been reached. The in-situ oil saturation measurements and the mass balance data were able to confirm the mean waterflood residual brine saturation, but recalibration of the level of adsorption was required. This recalibration was successfully achieved by adjusting the level of adsorption so the mean in-situ saturation data matched the produced fluids observed in the visual cell. The final adsorption was equivalent to a brine saturation of 0.11 which was similar to that observed during the initial trial. The overall uncertainty in mean in-situ gas saturation was estimated to be about ±5 % of the saturation measurement.

In an attempt to avoid the large changes in Cs^{137} adsorption experienced during Experiment 2, the brine was saturated with CO_2 during the ambient core conditioning phase of Experiment 3. The resulting pH was measured to be 6.5. Unfortunately, the CO_2 flooding was not sufficient to prevent the variation of tracer adsorption experienced in Experiment 2.

The brine pH is known to have a strong effluence on wettability and thresholds for switching from water-wet to oil-wet vary in the pH range 2-8 [7, 8]. The thresholds for the Miller and Brae systems were not known and it was decided that in Experiment 4 the active brine would not be introduced until the ageing was complete and a stable reservoir condition wettability had been achieved. It was hoped that this would also ensure stable adsorption of the Cs^{137}. The flooding protocol was revised so that the active brine was not introduced until the secondary waterflood when stable reservoir conditions had been established. Extensive flooding was necessary to ensure that the connate brine and injected brine reached a uniform specific activity. Again, the mean level of adsorption was established by fitting the mean in-situ brine saturation data to the produced brine measurements. The mean level of adsorption in this conglomerate core was estimated to be equivalent to a brine saturation of about 0.82. The distributed porosity/pore volume was determined independently of the gamma-emission measurements (see below) and by referring to the in-situ oil saturation measurements, the distributed brine tracer adsorption was deduced. This revised procedure successfully enabled distributed three-phase in-situ saturation measurements to be made. Again, the overall uncertainty in in-situ gas saturations was estimated to be about ±5 % of the saturation measurement.

3.4 In-Situ Porosity Measurement

The porosity distribution in Experiment 4 was measured using a gamma-attenuation technique [6] at ambient conditions. A dedicated facility was used and the procedure was as follows:

(a) Core scanned at 1 mm steps using gamma-attenuation to establish the location of the core ends
(b) Core gas volume determined by compressibility measurement
(c) Core scanned at 5 mm steps
(d) Core flooded from bottom to top with formation brine doped with 3% sodium iodide and the dispersion profile was measured and pore volume determined
(e) Core scanned at 5 mm steps

(f) Core flooded from bottom to top with undoped formation brine and the dispersion profile measured and pore volume determined
(g) Core scanned at 5 mm steps
(h) Core gas volume determined by compressibility measurements

A typical dispersion profile when the doped brine was flooded through the core is shown in Figure 1. It can be seen that the doped brine saturation reached a stable level and the displaced volume of undoped brine matched the pore volume from material balance. This result indicated that all of the pore volume had been accessed by the doped brine and that there was no adsorption of the dopant. The absolute porosity variation along the core was determined by using the following equation:

$$ f_i = \frac{\ln I_{Ui} - \ln I_{Di}}{\sum_{i=1}^{j} (\ln I_{Ui} - \ln I_{Di})} \cdot f_{av} $$

The resulting absolute porosity distribution is presented in Figure 2. The spatial resolution of the gamma-emission in-situ measurement made on the Depressurisation Rig was 30 mm and the local pore volumes determined by the gamma-attenuation data had a higher spatial resolution of 5 mm. It was therefore necessary to sum the local pore volume values measured by the gamma-attenuation method over a 30 mm interval and the resulting pore volume distribution is presented in Figure 3.

3.5 In-Situ Saturation Data

During the depressurisation phase it was necessary to allow for the oil shrinkage when converting gamma intensity into saturation. Direct measurements of oil specific activity as a function of pressure were made for the Miller live oil and these demonstrated that no $C_{10}H_{10}Fe$ partitioned into the gas. Tuned equations of state for the live oils were used to estimate the variation of specific activity with pressure.

In-situ measurements showing the variation of brine, oil and gas saturations during the depressurisation stage of Experiment 4 are shown in Figures 4 to 6. It can be seen that the oil saturation decreased uniformly with pressure and most of this saturation change was due to oil shrinkage; only 1.4% of the waterflood residual oil was produced. As pressure declined, the gas saturation increased throughout the core with the highest levels near the top of the core where the brine correspondingly reduced. The butt between the two core plugs has made a small impact on the fluid distributions. The in-situ saturations were used to determine the critical gas saturation and constrain the fit during numerical simulation of the coreflood.

4. LEAK INTEGRITY

4.1 Core Sleeve

The presence of high concentrations of CO_2 in the test fluids precluded the use of elastomer sleeves and epoxy resin coated cores. The gas would have diffused through such sleeves and become lost to the annulus fluid. Reduction in the level of CO_2 in the core fluids would have resulted in an unacceptable change in the composition and phase behaviour. Therefore a core sleeve was needed that was both impermeable to gas and had a low gamma-attenuation coefficient.

A practical solution was developed which used an outer sleeve of aluminium tube and an inner sleeve of PTFE which provided a liquid barrier to prevent the brine corroding the outer aluminium sleeve. The end platten distribution plates were designed so that "O" ring seals prevented annulus fluid from entering the core and also prevent core fluid from coming into contact with the outer aluminium sleeve. A clamping arrangement was designed to ensure that the outer sleeve compressed on to the "O" rings. Figure 7 shows a schematic of the sleeving arrangement. This sleeving arrangement proved to be very successful and had the following benefits:

- Extremely leak-tight
- Very robust with respect to pressure excursions
- Cores can be reused or re-sleeved
- Low attenuation to gamma or x-rays
- Compatible with solvents

4.2   Circuit Design and Testing

The experiments were conducted in a high pressure rig constructed from mainly Hastelloy and other corrosion resistant materials and the design conditions were 691 bara and 150°C. In these experiments the maximum conditions used were 415 bara core circuit (484 bara annulus circuit) and 123°C.

A simplified flow circuit is presented in Figure 8. It consisted of a vertical core holder, visual cell, separator vessel and two parallel extraction circuits, all housed within a large temperature controlled oven. Each extraction circuit comprised a 15 mL sample vessel into which the visual cell fluids were withdrawn and a 500 mL gas vessel into which the nitrogen from the gas spring was collected. Flow rate was controlled by extracting fluid using alternate sides of a twin barrelled constant volume extraction pump. The ultra-low depressurisation rates required in these experiments were achieved by using the extraction pump in conjunction with a large nitrogen gas spring in the core outlet circuit to control fluid extraction from the core. This arrangement enabled extraction rates of 0.3 mL day^{-1} for the longest depressurisation period of 141 days to be realised. Pressures and temperatures around the circuit were recorded using a data logging system.

During these depressurisation experiments it was very important that the core circuit was extremely leak tight. The relatively small hydrocarbon pore volumes at the start of the depressurisation stage of between 10 and 36 mL meant that if a leak occurred then it could have had a significant effect on the measurement of produced fluids collected in the visual cell. A great deal of effort was spent to ensure that the leak rates were as low as could reasonably be achieved. The rig was designed with a minimum number of valves and connections in critical parts of the circuit. Extensive leak testing was performed by pressurising the circuits with gas and monitoring the pressure variation in parts of the circuit together with variation in temperature to demonstrate that leak rates were acceptable.

Subsequent tests were performed both before and after raising the rig to full test conditions, with the rig filled with brine and oil. These tests confirmed that leak rates in critical parts of the circuit were as low as 0.008 mL day^{-1} at full test conditions. The leak rate was determined using the following equation by measuring the change in pressure with time, and measuring the compressibility of the system:

$$\frac{\Delta V}{\Delta t} = \frac{\Delta P}{\Delta t} \cdot C$$

The oven and room temperature were controlled to ±0.3°C and ±2°C respectively, however the due to the incompressible nature of these fluids, the effect of temperature had to be taken into account when assessing the leak rate. Figure 9 presents a typical variation of pressure and temperature with time in the core when filled with brine at room temperature. It can be seen that careful analysis is required in order to eliminate the effects of temperature variation. With typical compressibilities, temperature control and accuracy of pressure measurement, it was necessary to continue these leak tests for at least 5 days in order to demonstrate adequate leak tightness.

During the latter stages of some of the experiments it was found that the leak rate into the core circuit from the overburden circuit had increased to as much as 0.067 mL day^{-1}. In those cases annulus fluid had entered the pipework between the core outlet and the visual cell via a ferrule on the connection pipe to the core outlet end platten. The in-situ saturation data were able to demonstrate that the leaks did not affect the core and thus this capability provided additional value to the experimental study.

5.   PRODUCED FLUID MEASUREMENTS

A calibrated visual cell was fitted with a piston and connected between the core outlet and the extraction circuit. The inclusion of the cell allowed fluids produced from the core to be measured and provide material balance checks and calibration reference points for in-situ saturation measurements.

In the early experiments it was found that the piston in the cell did not move during the depressurisation stage. It was considered that the pressure drop was insufficient to overcome the static friction of the piston, and in those cases the produced fluid by-passed the piston.

To overcome this problem another fluid was required that was more dense and immiscible with brine. Traditionally mercury is used in such applications, however due to the safety and environmental implications the use of mercury was not an attractive option. After some research, a fluorinated hydrocarbon liquid, Flutec PP9 [9] was identified. This fluid was inert, non-toxic, non-polar and denser than brine by a factor of almost two. It enabled the volume of the brine produced during the depressurisation stage to be measured.

The PP9 was introduced into the visual cell at the end of the secondary waterflood stage, just prior to the depressurisation. The only disadvantage of using the PP9 was that it could adsorb gas, much like water. It was therefore necessary to gas-up the PP9 with the correct amount of CO_2 before it was placed in the visual cell to ensure that it was in equilibrium with the carbonated brine that was produced from the core.

6.   DETERMINATION OF CRITICAL GAS SATURATION AND RELATIVE PERMEABILITIES

6.1   Critical Gas Saturation

Critical gas saturation is often defined as the point at which gas begins to leave the core. In experiments that do not have the benefit of in-situ gas saturation reliance has to be made on observations from a visual cell. If the volume of pipework connecting the core to the cell is large and the positioning of the cell and geometry of the pipework is not favourable, then this can result in significant delay in seeing the arrival of gas in the cell which in turn can lead to large uncertainties in the determination of the critical gas saturation.

In-situ saturation measurements provide a much more reliable means of determining the critical gas saturation and can give an insight into where gas is moving within the core. To determine the critical gas saturation, it was necessary to compare the measured in-situ saturation data with the value that would occur if no gas flowed out of the core. Departure of the measured gas saturation profile from the "no-gas-flow" saturation profile indicated the point at which gas left the core; i.e. the critical gas saturation.

The "no-gas-flow" saturation values have been determined by assuming that a cumulative volume of gas built up in the core from depressurising the oil, and that this gas stayed behind in the core as the liquids were ejected. To calculate the volume of gas, constant composition expansion data from a tuned equation of state model for the particular reservoir fluid have been used to determine the volumes of hydrocarbon gas associated with the oil, before the oil was removed from the core.

The following scheme has been used to determine the individual cumulative volumes of hydrocarbon gas associated with the oil leaving the core. The individual components have then been summed to give the overall gas volume and converted into saturations by dividing by the appropriate local pore volume. The cumulative volume of hydrocarbon gas has been calculated as follows:

$$V_{ghc} = \sum_{m=0}^{n} \left[\left((V_{hcsat})_m \times \left(\left(\frac{v_{ghc}}{V_{hcsat}} \right)_{m+1} - \left(\frac{v_{ghc}}{V_{hcsat}} \right)_m \right) \right) \right]$$

This scheme can also be applied to discrete intervals within the core to enable critical gas saturations to be determined locally.

Figure 10 presents the results from Experiment 4 showing the departure of the measured gas saturation from the "no-gas-flow" line for the whole core. It can be seen that the mean critical gas saturation was approximately 0.025. Figures 11 and 12 present the local in-situ gas saturations and "no-gas-flow" lines for positions 375 and 45 mm from the top of the core respectively. Figure 11 shows that gas was leaving the bottom of the core at saturations of about 0.02, but for pressures below 150 bara, about half of the gas was trapped in the core. Figure 12 shows that the rate of arrival of gas exceeded the rate of departure at pressures between 175 and 90 bara and the total gas saturation was greater than the "no-gas-flow" line. It should be noted in Experiment 4 that despite a relatively extensive depressurisation to 70 bara, only 30% of the available gas was produced.

6.2 Derivation of Relative Permeabilities

A simulation model was constructed for Experiments 2-4 and a match of measured pressures and in-situ saturations was sought by altering the relative permeability and capillary pressure data. It would appear that the *average* saturations could be modelled by a range of relative permeability/capillary pressure inputs, but it was found that the uncertainty associated with these fitted parameter was much reduced when seeking a fit to the *distributed* in-situ saturation data. A detailed description of the simulation results is beyond the scope of this paper, but improved accuracy of relative permeabilities is a significant benefit of the in-situ saturation data.

7 CONCLUSIONS

This paper describes the experimental methods which have been developed during what may be the most representative depressurisation experiments that have been conducted to date. Great effort has been expended in ensuring that the key parameters were correctly represented in the reservoir condition experiments. The experiments were conducted at pressures up to 415 bara and 123°C using reservoir core and fluids.

Particular challenges related to the high CO_2 content of the oil and the low flow rates anticipated during these studies. The low flow rates required relatively high levels of leak tightness and a new core sleeving method and testing protocol were developed which yielded acceptable leak rates. Another consequence of the low flow rates was that the pressure drop was not sufficient to overcome the static friction in the piston of a standard high pressure/temperature visual cell used for monitoring produced volumes. As an alternative to mercury, a fluorinated hydrocarbon liquid was developed for use as a 'liquid-piston'.

In order to assess the impact of core artifacts and generate relative permeability data, three-phase in-situ saturation measurements have been conducted. As a result of a series of compatibility trials, a successful combination of radiotracers and experimental procedure has been established. These measurements provided a means of determining critical gas saturations and relative permeabilities which can be used in reservoir simulations.

NOMENCLATURE

C	Compressibility
V_{ghc}	Cumulative volume of hydrocarbon gas
v_{ghc}/V_{hcsat}	Expansion factor for hydrocarbon gas at pressure interval from constant composition expansion (CCE) data
V_{hcsat}	Equivalent volume of hydrocarbon fluid (at saturation pressure) in the core determined from in-situ saturation oil volume measurement and CCE data
f	Absolute Porosity
I_D	Intensity of gamma radiation passing through doped material
I_U	Intensity of gamma radiation passing through undoped material
DP	Pressure change
DV	Volume change
Dt	Time interval

Subscripts

av	Average value from material balance
i	In-situ saturation measurement interval
j	Final in-situ saturation measurement interval
m	Pressure decrement, starting at bubble point pressure, m=0
n	Final pressure decrement

ACKNOWLEDGEMENTS

REFERENCES

1. McPhee, C., "Realising Value from SCAL," Dialog Newsletter of the London Petrophysical Soc., Vol 7, Issue 1, February 1999.
2. Whattler P.R., "Increasing the Value of Core Analysis," Proc. 2nd European SCA Symp., pp 53-76, London, 22-24 May 1991.
3. Naylor P., Fishlock T.P., Mogford D.J., Smith R.A., "Relative Permeability Measurements for Post-Waterflood Depressurisation of the Miller Field, North Sea," SPE 63148, Annual Tech. Conf and Exhibition, Dallas, Texas, 1-4 October 2000.
4. Hawes R.I., Dawe R., Naylor P., Tehrani D., "Engineered Depressurisation of Waterflooded Reservoirs", Advances in Reservoir Technology Conference, London, 7-8 November 1994.
5. Bailey N.A., Rowland D.P., Robinson D.P., "Nuclear Measurements of Fluid Saturation in EOR Experiments", Proc. Euro. Symp of EOR, pp 483-498, Bournemouth, 21-23 September 1981.
6. Naylor P., Puckett D.A., "In-Situ Saturation Distributions: The Key to Understanding Core Analysis", SCA-9405, Int. Symp. SCA, Stavanger, Norway, 12-14 September 1994.
7. Morrow N., "Wettability and its Effect on Oil Recovery", JPT, pp1476-1484, December 1990.
8. Anderson W.G., "Wettability Literature Survey-Part 1: Rock/Oil/Brine Interactions and the Effects of Core Handling on Wettability", JPT, pp 1125-1144, October 1986.
9. Flutec PP9 Perfluorocarbon, F2 Chemicals Ltd, Lea Lane, Lea Town, Preston, Lancashire, PR4 ORZ, UK.
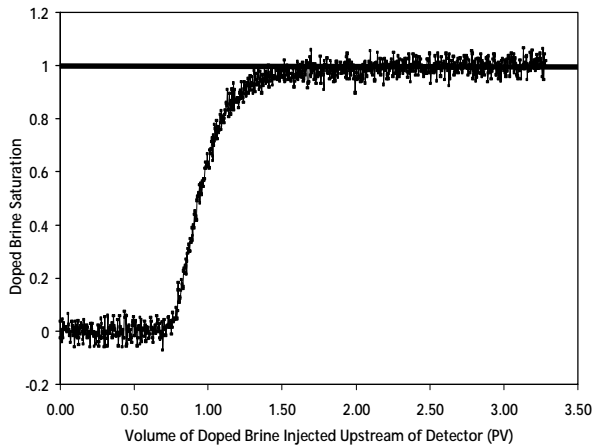
Fig 1: Doped Brine Dispersion Profile Exp 4
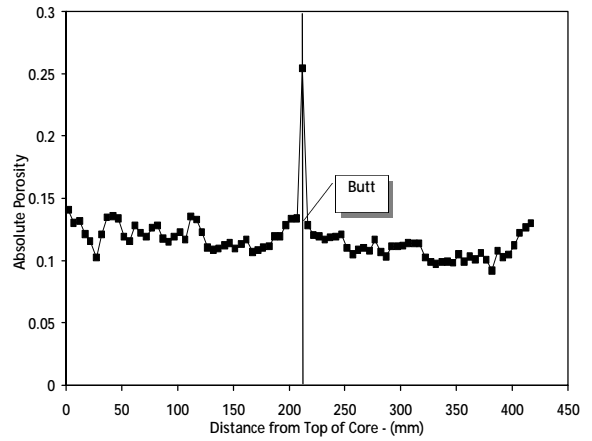
Fig 2: Porosity Distribution Exp 4
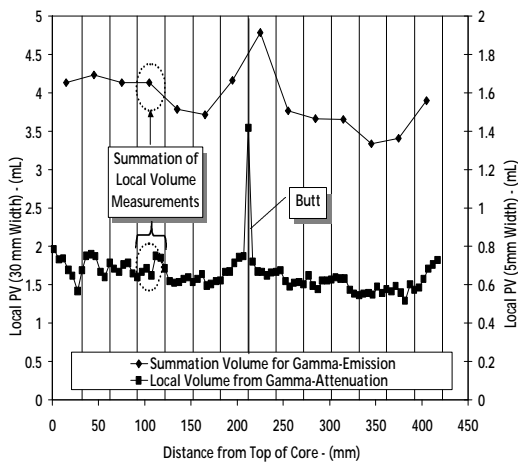
Fig 3: Local Pore Volume Distribution Exp 4
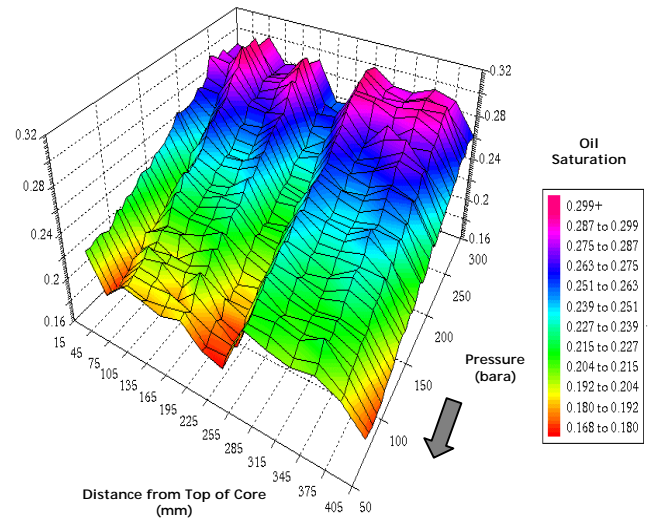
Fig 4: Oil Satn During Depressurisation Exp 4
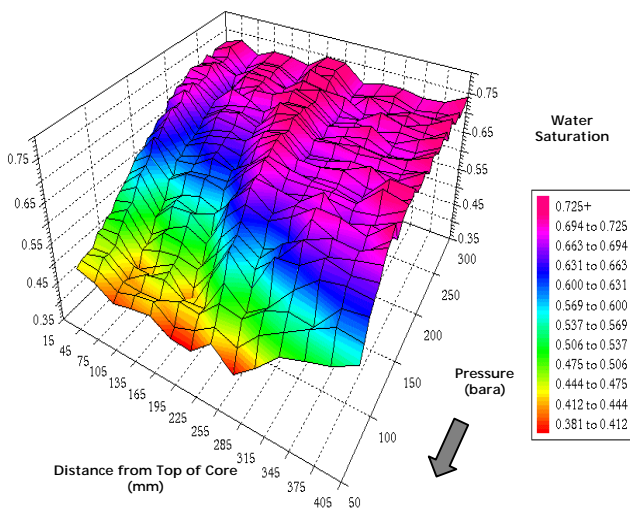
Fig 5: Water Satn During Depressurisation Exp 4
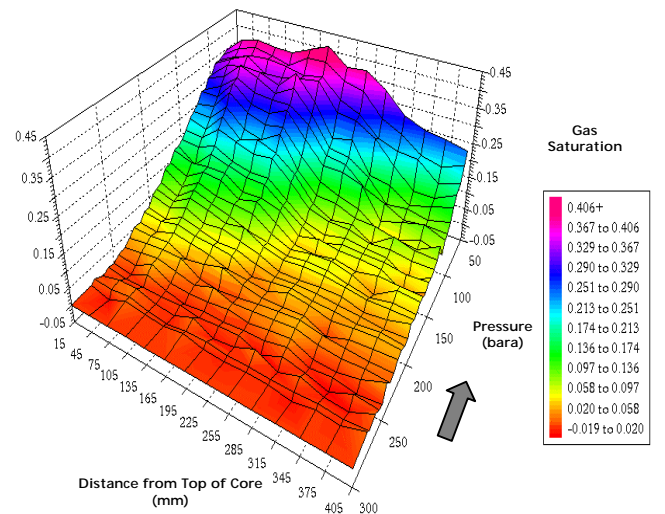
Fig 6: Gas Satn During Depressurisation Exp 4
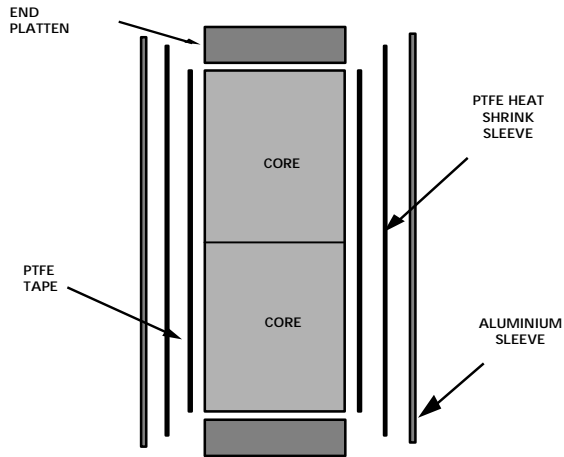
Figure 7: Core Sleeve Arrangement
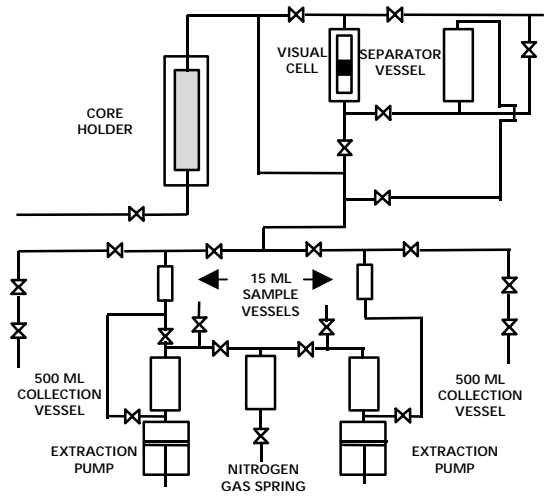
Figure 8: Depressurisation Rig Flow Circuit
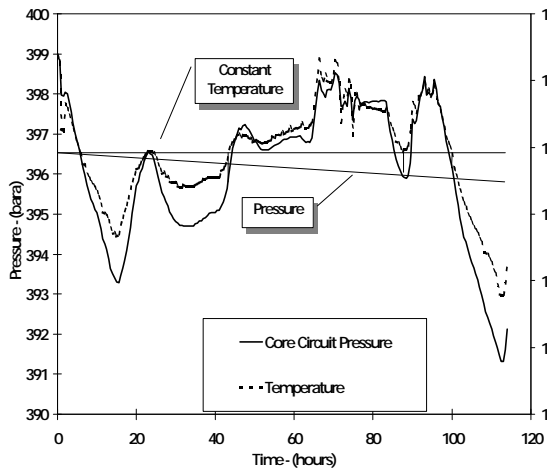
Figure 9: Typical Leak Test Data
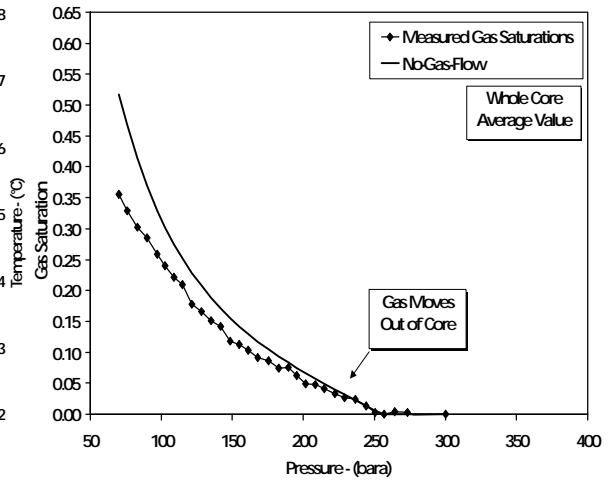
Figure 10: Exp 4 Critical Gas Saturation (Mean)
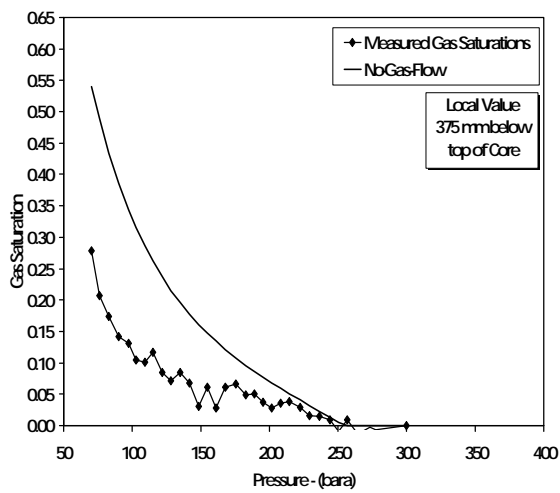
Figure 11: Exp 4 Gas Saturation (375 mm)
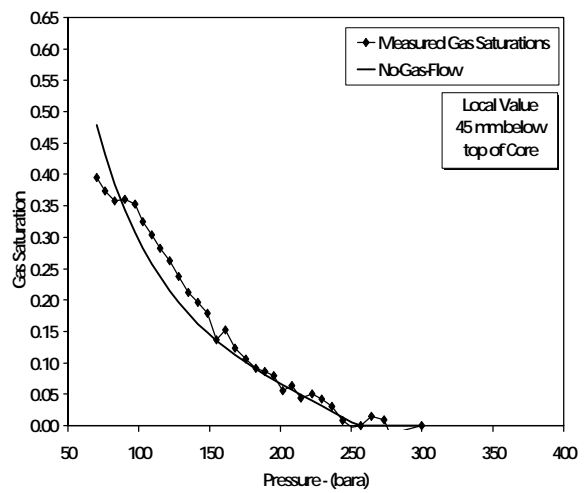
Figure 12: Exp 4 Gas Saturation (45 mm)